HIGH RESOLUTION 3-D IMAGING VIA SQUINT SAR AND FORWARD-LOOKING SAR

Liang Xu[1] , Weihai Li[2], Kai Tan[3], Tonghuan Yu[4]
Key Laboratory of Electromagnetic Space Information, Chinese Academy of Sciences,
School of Information Science and Technology, University of Science and Technology of China
No.96, JinZhai Road Baohe District,Hefei,Anhui, 230026,P.R.China.
[1]Email: xulian@mail.ustc.edu.cn
[2]Email: whli@ustc.edu.cn
[3]Email: tansk@mail.ustc.edu.cn
[4]Email: yth099@mail.ustc.edu.cn

KEY WORDS: SAR, 3-D, forward-looking, squint, RCMC

ABSTRACT:

In this paper, we introduce a high resolution 3-D imaging method by combining squint airborne synthetic aperture radar(SAR) and forward-looking SAR. As conventional SAR image is the projection of 3-D targets on a 2-D plane, the third dimension information could not be obtained without multi-pass or multi-antenna. Squint airborne SAR can obtain high resolution 2-D image of the anterolateral terrain, while forward-looking SAR could be utilized to achieve the 3-D imaging of the terrain ahead. It is sufficient to cover the low along-track resolution of forward-looking SAR through this method. Furthermore, the multi-antenna of forward-looking SAR is no longer needed which greatly reduce the cost of imaging. Since the antenna of squint SAR and forward-looking SAR pointing forward, their echo characteristics have great similarities. Imaging algorithm proposed for squint SAR is also suitable for forward-looking SAR. In this algorithm, a linear range cell migration(RCMC) is performed to correct the titled spectrum of the raw data and an azimuth demodulation is taken to move the spectrum in the baseband. Point scatter simulation is carried out to verify the 3-D imaging algorithm. Simulation results, such as five point scatters, show that we could acquire the correct value of point scatters in range, and which confirms the validity of this method.

1. INTRODUCTION

SAR is a kind of active and coherent microwave imaging radar(Ian G Cumming and Frank Hay-chee Wong, 2005). Unlike other imaging radar, SAR has the characteristics of all day night, all-weather working and high resolution imaging, which make SAR have an important position in imaging radar and great applications in many areas such as topography and military reconnaissance. However, with the development of high speed digital chip and digital signal processing algorithm, only high resolution 2-D imaging cannot be used to the 3-D mapping, which limits the further development of SAR.

Generally speaking, there are five kinds of SAR which have the capability of 3-D imaging. They are interferometry SAR(Lideng Wei, Songtao Han, and Maosheng Xiang, 2010), polarimetric SAR, curvilinear SAR, tomography SAR(John Homer, ID Longstaff, Zhishun She, and Doug Gray, 2002), (P Berardino, G Fornaro, R Lanari, E Sansosti, F Serafino, and F Soldovieri, 2002) and forward-looking SAR(Yang Ruliang, Tan Lulu, and Ren Xiaozhen, 2009), (Qi Chen and RL Yang, 2008), (Xiaozhen Ren, Jiantao Sun, and Ruliang Yang, 2011), in which the latter two have the most extensive application. Tomography SAR obtains several two dimensional images of the interested terrain in different baselines, which compose a large aperture on the elevation direction. There are no differences between conventional SAR and tomography SAR for azimuth and range imaging. That is to say, tomography SAR can acquire high resolution in azimuth and range dimension. However, the elevation dimensional resolution of tomography is limited by the length of aperture in the elevation direction. If we want to improve the elevation dimensional resolution, according to the spatial Nyquist sampling theorem, we must add the number of baseline, which greatly increase the cost of imaging.

The high resolution of forward-looking SAR in along track direction is generally obtained by focusing a transmitted large bandwidth linear frequency modulated pulse, whereas high resolution in elevation direction is achieved by synthesizing a large aperture. The resolution in cross track direction is realized by the array antennas on the plane's wing. Due to the limitation of the length of wing and the number of antenna, the resolution in cross track direction is very low. Besides, array antennas increase the complexity of imaging.

Since forward-looking SAR can obtain high resolution image of the front area in along track and elevation direction with one antenna and one flight, squint SAR(Tonghuan Yu and Weihai Li, 2015) could compensate the low cross track resolution weakness of forward-looking SAR. The principle of three-dimensional imaging is analyzed in the next section. Section 3 gives the algorithm adapt to both squint SAR and forward-looking SAR. Section 4 gives the simulation results and error analysis. The last section is the conclusion.

2. THE PRINCIPLE OF 3-D IMAGING

2.1 Data Acquision in Azimuth and Range

Squint SAR data acquisition model in stripmap mode SAR is depicted in Fig.1, in which x axis is the azimuth(along track) and y axis is defined as the range(cross track). α and β, respectively, denote the squint angle and elevation angle. P_A is the center of beam footprint, and is also the center of swath. P is a 3-D point target to be imaged in the swath with height h, and P_1 is the vertical projection of P in the ground plane. P_2 is a point whose azimuth coordinate is same as P's, while its range coordinate is the result of P's range coordinate minus h. The focusing position of the 3-D target in 2-D imaging is same as the focusing position of P_2. That is say, as long as we obtain the 2-D coordinate of P_2, the position of P in range and azimuth could be acquired.

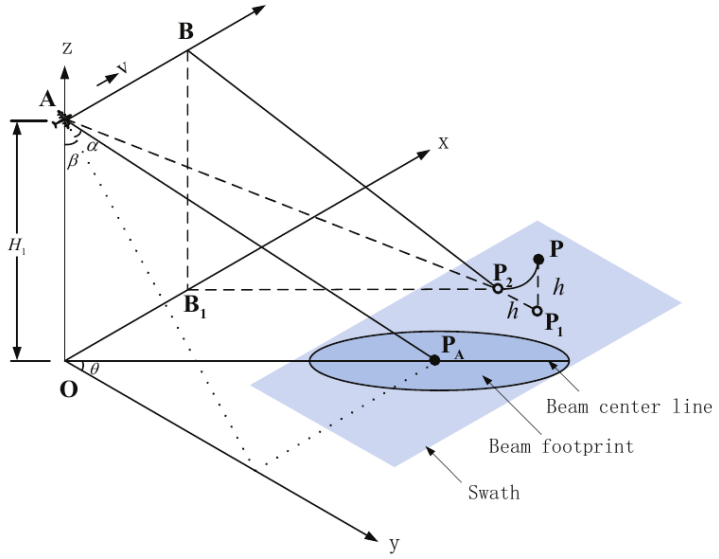

Figure 1. The geometry of squint SAR.

When the aircraft travels from A to B, the beam center line in the ground plane just past through P_2. According to the triangle OB_1P_2, the hyperbolic equation of the range history of P_2 can be written as

$$r(\eta;r_c,\alpha_c)=\sqrt{r_c^2+v^2(\eta-\eta_c)^2-2v(\eta-\eta_c)\sin\alpha_c} \tag{1}$$

where η is the azimuth time, η_c is the azimuth time when the beam center just pass through P_2, r_c and α_c, respectively, are the instantaneous slant range and the angle between slant range and plane of zeros Doppler at η_c.

Expanding (1) at $\eta=\eta_c$ to its Taylor series and keeping the Taylor expansion up to the second order term, then we have

$$\begin{aligned} r(\eta;r_c)\approx{} & r_c- \\ & v\sin\alpha_c(\eta-\eta_c) \\ & +\frac{v^2\cos^2\alpha_c}{2r_c}(\eta-\eta_c)^2+\cdots \end{aligned} \tag{2}$$

According to (2), the Doppler centroid and Doppler rate in squint mode SAR can be expressed as

$$f_{\eta_c}(\alpha_c) = \frac{2v\sin\alpha_c}{\lambda} \tag{3}$$

$$k_a(\alpha_c) = \frac{2v^2\cos^2\alpha_c}{\lambda r_c} \tag{4}$$

where λ is the wavelength.

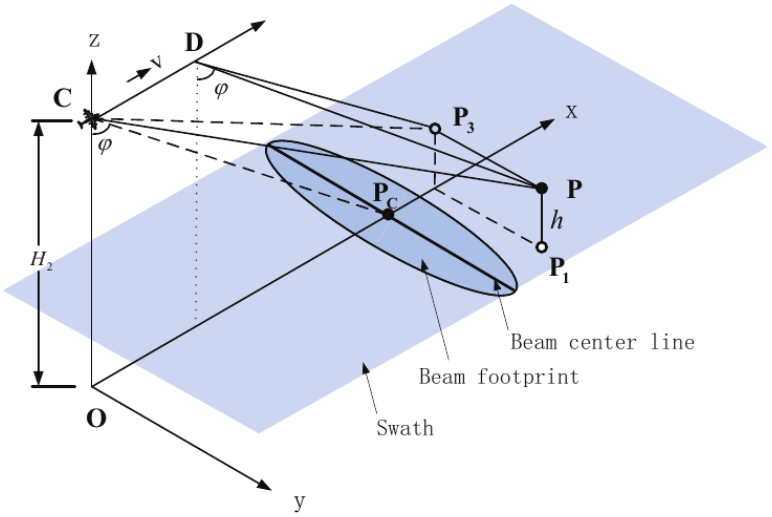

Figure 2. The geometry of forward-looking SAR.

2.2 Data Acquision in Azimuth and Elevation

Forward-looking SAR data acquisition model is show in Fig. 2, in which x and y axis, respectively, are the along track and cross track direction. φ is the elevation angle. P_C is the center of beam footprint, and is also the center of swath. P_3 is the vertical projection of P in the x-z plane. As the aircraft travels along a straight line parallel to the x axis with a const velocity v, the beam footprint sweeps along the ground. When the aircraft arrives at D, the beam center line just past through P. According to the triangle CDP, the hyperbolic equation of the range history of P can be written as

$$r(\eta; r_c, \varphi_c) = \sqrt{r_c^2 + v^2(\eta - \eta_c)^2 - 2v(\eta - \eta_c)\sin\varphi_c} \tag{5}$$

where η_c is the azimuth time when the beam center just pass through P, r_c and φ_c, respectively, are the instantaneous slant range and the angle between slant range and y-z plane at η_c. The range history expression in forward-looking SAR seems quite similar to the range history expression in squint SAR by contrast (1) with (5), except for the angle α_c and φ_c. Therefore, the range history in both squint SAR and forward-looking SAR can be rewritten as

$$r(\eta; r_c, \phi_c) = \sqrt{r_c^2 + v^2(\eta - \eta_c)^2 - 2v(\eta - \eta_c)\sin\phi_c} \tag{6}$$

where ϕ_c is the angle α_c or φ. Expanding (5) at $\eta = \eta_c$ to its Taylor series, then the Doppler parameters in forward-looking SAR can be expressed as

$$f_{\eta_c}(\varphi_c) = \frac{2v\sin\varphi_c}{\lambda} \tag{7}$$

$$k_a(\varphi_c) = \frac{2v^2 \cos^2 \varphi_c}{\lambda r_c} \tag{8}$$

3. THE ALGORITHM OF 3-D IMAGING

The flowchart of three-dimensional imaging algorithm is shown in Fig. 3. If the raw SAR data comes from squint SAR, the value of ϕ in filter H_1 and H_2 will be set as α, and we will get the final imaging in azimuth and range. If the raw SAR data comes from forward-looking SAR, the final imaging in azimuth and elevation will be obtained by setting the value of ϕ to φ.

Assuming both of the squint SAR and forward-looking SAR transmit a linear FM signal, and the demodulated echo signal from P is given by

$$\begin{aligned} s(\eta, \tau; r_c, \phi_c) = w_r[\tau - \frac{2r(\eta; r_c, \phi_c)}{c}] w_a(\eta - \eta_c) \\ \times exp\{ j\pi k_r (\tau - \frac{2r(\eta; r_c, \phi_c)}{c})^2 \} \\ \times exp\{ -j \frac{4\pi}{\lambda} r(\eta; r_c, \phi_c) \} \end{aligned} \tag{9}$$

where $w_a(\eta)$ is the azimuth envelope, c is the speed of light. The meaning of τ, k_r and $w_r(\tau)$ are determined by the value of ϕ_c. If the value of ϕ_c is α_c, (9) will be the echo data of squint SAR. τ and k_r, respectively, are the range time and range chirp rate, and $w_r(\tau)$ is the range envelope. Otherwise, (9) is the echo data of forward-looking SAR. τ, k_r and $w_r(\tau)$ are the parameters in elevation.

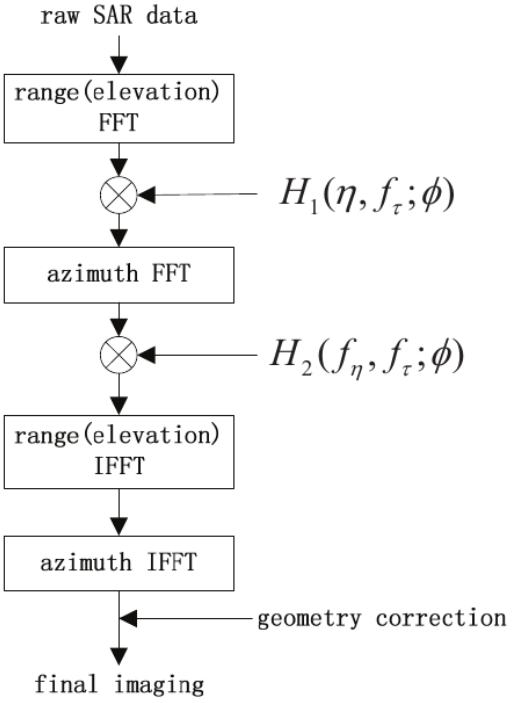

Figure 3. Flowchart of 3-D imaging algorithm.

Applying the range(elevation) FFT to (9) yield

$$S(\eta, f_\tau; r_c, \phi_c) = W_r(f_\tau) w_a(\eta - \eta_c) \times exp\{-j\frac{\pi}{k_r} f_\tau^2\} exp\{-j\frac{4\pi r(\eta; r_c, \phi_c)}{c} f_\tau\} \times exp\{-j\frac{4\pi}{\lambda} r(\eta; r_c, \phi_c)\} \quad (10)$$

where $W_r(f_\tau)$ represents the range(elevation) frequency envelope.

According to (9), the filter H_1 can be set up as

$$H_1(\eta, f_\tau; \phi) = exp\{j\frac{\pi}{k_r} f_\tau^2\} exp\{-j\frac{4\pi v \sin\phi}{c}\eta f_\tau\} \times exp\{-j2\pi\eta f_{\eta_c}(\phi)\} \quad (11)$$

The first exponential term in (11) is used to realize the range(elevation) compression. Another two exponential terms, respectively, are the linear RCMC and azimuth demodulation.

Multiplying (11) with (10) and transforming the result into 2-D frequency domain get the signal

$$S_1(f_\eta, f_\tau; r_c, \phi_c) \approx W_r(f_\tau) W_a(f_\eta) \times exp\{-j\frac{4\pi(r_c + v\eta_c \sin\phi_c)}{c} f_\tau\} \times exp\{-j\frac{\lambda^2 r_c}{2cv^2\cos^2\phi_c} f_\eta^2 f_\tau\} \times exp\{-j\pi\frac{f_\eta^2}{k_a}\} \quad (12)$$

where $W_a(f_\eta)$ represents the range frequency envelope. In order to get the final image, filter H_2 can be set up as

$$H_2(f_\eta, f_\tau; \phi) = exp\{j\frac{\lambda^2 R_c}{2cv^2\cos^2\phi} f_\eta^2 f_\tau\} exp\{j\pi\frac{f_\eta^2}{k_a(\phi)}\} \quad (13)$$

Table 1. System parameters

SAR mode	squint	forward-looking
wavelength	0.1m	0.1m
range chirp rate	100MHz/ μs	100MHz/ μs
range chirp duration	1.5μs	1.5μs
platform altitude	3km	800m
platform velocity	150m/s	150m/s
real aperture length	2m	2m
PRF	127Hz	91Hz
squint angle	45°	/
elevation angle	45°	60°

Multiplying (13) with (12) and transforming it to 2-D domain gets the focused image

$$s_1(\eta, \tau; \phi_c) = sinc\{\Delta f_a(\eta - \eta_c)\} \times sinc\{\Delta f_r[\tau - \frac{2(r_c + v\eta_c \sin\phi_c)}{c}]\} \quad (14)$$

where Δf_a and Δf_r are the azimuth and range(elevation) bandwidth, respectively. According to (14), we can know the coordinate of focal position is (a, r, e), where

$$a = v\eta_c \tag{15}$$

$$r = r_c + v\eta_c \sin\alpha_c \tag{16}$$

$$e = r_c + v\eta_c \sin\varphi_c \tag{17}$$

In order to transform it to the correct position, the geometry correction is necessary. The correct position of 3-D target P is (a', r', e'), where

$$a' = (r - a\sin\alpha)\sin\alpha + a \tag{18}$$

$$r' = (r - a\sin\alpha)\cos\alpha \tag{19}$$

$$e' = H_2 - (e - a\sin\varphi)\cos\varphi \tag{20}$$

4. SIMULATION RESULTS

In this section, point scatter simulation is carried out to verify the 3-D imaging algorithm via squint SAR and forward-looking SAR. The main system parameters used for simulation are listed in Table 1. Five point scatters, which located at (4263,2950,30), (4283,3000,10), (4243,3000,0), (4203,3000,40), (4223,3050,20) are simulated. The spatial position of the five points are shown in Fig. 4.

The simulation results are shown in Fig. 5. As conventional 2-D SAR image is the projection of 3-D targets on a 2-D plane, the value of range in Fig. 5(a) is not equal to its real value. However, according to Fig. 5(b), we could acquire the real value of point scatters in range. From Fig. 5 we can know all the point scatters are well focused.

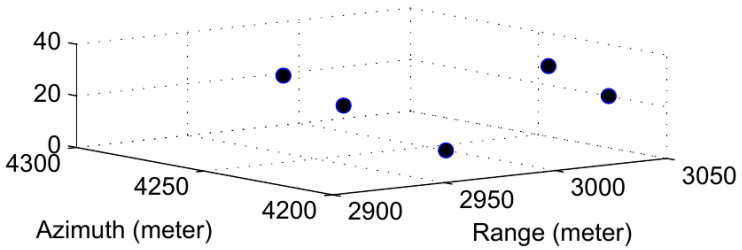

Figure 4. Spatial position of point scatters.

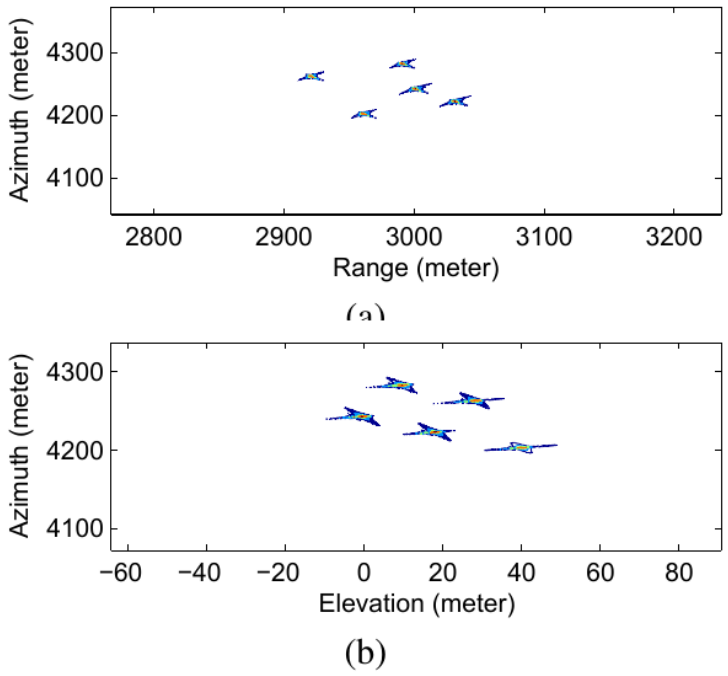

Figure 5. Point scatters simulation results. (a) Imaging in azimuth and range. (b)Imaging in azimuth and elevation.

5. CONCLUSION

In this paper, a high resolution 3-D imaging method via squint SAR and forward-looking SAR has been introduced. Here we utilize squint airborne SAR to obtain high resoltion 2-D image of the anterolateral terrain, and utilize forward-looking SAR to achieve the third dimensional imaging. With this method, the along-track resolution has been improved and the cost of imaging has been greatly reduced compared with forward-looking SAR. Furthermore, since the antenna of squint SAR and forward-looking pointing forward, their echo characteristics seem quite similar. We can utilize one algorithm to process two echo data. The simulation results confirm the validity of the proposed 3-D imaging method.

6. REFERENCES

[1] Ian G Cumming and Frank Hay-chee Wong, 2005. Digital processing of synthetic aperture radar data: algorithms and implementation, Artech house.

[2] John Homer, ID Longstaff, Zhishun She, and Doug Gray, 2002."High resolution 3-d imaging via multi-pass sar," IEE Proceedings-Radar, Sonar and Navigation, vol. 149, no.1, pp. 45–50.

[3] Lideng Wei, Songtao Han, and Maosheng Xiang, 2010. "Processing for airborne interferometric sar data with high squint," in Geoscience and Remote Sensing Symposium(IGARSS), 2010 IEEE International. IEEE, pp.4668–4670.

[4] P Berardino, G Fornaro, R Lanari, E Sansosti, F Serafino, and F Soldovieri, 2002."Multi-pass synthetic aperture radar for 3-d focusing," in Geoscience and Remote Sensing Symposium, IGARSS'02. 2002 IEEE International. IEEE, 2002, vol. 1, pp. 176–178.

[5] Qi Chen and RL Yang, 2008. "Research of chirp scaling imaging algorithm for air-borne forward-looking sar," Journal of Electronics & Information Technology, vol. 30, no. 1, pp. 228–232.

[6] Tonghuan Yu and Weihai Li, 2015. "A high squint airborne sar imaging algorithm with low prf," in Signal and Information Processing (ChinaSIP), 2015 IEEE China Summit and International Conference on. IEEE, pp. 1076–1080.

[7] Xiaozhen Ren, Jiantao Sun, and Ruliang Yang, 2011. "A new three-dimensional imaging algorithm for airborne forward-looking sar," IEEE Geoscience and Remote Sensing Letters, vol. 8, no. 1, pp. 153–157.

[8] Yang Ruliang, Tan Lulu, and Ren Xiaozhen, 2009. "Research of three-dimensional imaging processing for air-borne forward-looking sar," in Radar Conference, 2009 IET International. IET, pp. 1–4.